Journal of Molecular and Cellular Cardiology 132 (2019) 36–48

Contents lists available at ScienceDirect

Journal of Molecular and Cellular Cardiology

journal homepage: www.elsevier.com/locate/yjmcc

Knockout of Canopy 2 activates p16^{INK4a} pathway to impair cardiac repair

Wenjuan Yin[a,b], Jian Guo[b], Chongyu Zhang[b], Faisal J. Alibhai[b], Shu-Hong Li[b], Phyllis Billia[b,c,e], Jun Wu[b], Terrence M. Yau[b,d], Richard D. Weisel[b,d], Ren-Ke Li[b,d,*]

[a] Department of Pathology, Shanxi Key Laboratory of Birth Defect and Cell Regeneration, Shanxi Medical University, Taiyuan, China
[b] Toronto General Hospital Research Institute, Division of Cardiovascular Surgery, University Health Network, Toronto, ON, Canada
[c] Division of Cardiology, University Health Network, Toronto, Canada
[d] Division of Cardiac Surgery, Department of Surgery, University of Toronto, Toronto, ON, Canada
[e] Department of Physiology, University of Toronto, Toronto, ON, Canada

ARTICLE INFO

Keywords:
Canopy 2
p16^{INK4a}
Myocardial infarction
Heart failure
Cardiac repair

ABSTRACT

Background: Cardiac repair depends on angiogenesis and cell proliferation. Previously we identified Canopy 2 (CNPY2) as a secreted angiogenic growth factor which promotes neovascularization. We investigated the role of CNPY2 in cardiac repair following myocardial infarction (MI) and the possible mediators involved using *Cnpy2* knockout (KO) mice and human cardiac tissue.

Methods and results: Cardiac tissue from patients with end-stage heart failure had significantly lower endogenous CNPY2 expression compared to samples from control patients. CNPY2 expression in mouse hearts significantly decreased following MI. Significantly less leukocyte and endothelial cell proliferation was found in *Cnpy2* KO than wild-type (WT) mice post MI which contributed to impaired angiogenesis, tissue repair, and decreased cardiac function (fractional shortening: WT: 21.1 ± 2.1% vs. KO: 16.4 ± 1.6%, $p < .01$ at day 28 post MI). RT-qPCR revealed significantly increased p16^{INK4a} expression in *Cnpy2* KO mouse hearts (WT: 1.0 ± 0.04 vs. KO: 2.33 ± 0.11 [relative expression of p16 ^{INK4a}], $p < .01$) which was confirmed by immunostaining (WT: 8.47 ± 1.22 vs. KO: 12.9 ± 1.22 [% total cells], $p < .05$) for the p16^{INK4a} protein. Expression of cell cycle-related proteins, cyclin D1, cyclin-dependent kinases 4 and 6, and phosphorylated retinoblastoma protein (pRb) was significantly decreased in *Cnpy2* KO mouse hearts. The up-regulation of the p16^{INK4a}/cyclin D1/Rb pathway by knockout of *Cnpy2* was accompanied by attenuation of PDK1/Akt phosphorylation. MI exacerbated the detrimental effects of p16^{INK4a} on tissue repair in *Cnpy2* KO mice. Overexpression of CNPY2 in the cardiac tissue of transgenic mice reversed the inhibition of cell proliferation through suppression of the p16^{INK4a} pathway.

Conclusions: Cardiac injury and progressive heart failure were associated with decreased CNPY2 levels in both humans and mice. Knockout of *Cnpy2* resulted in up-regulation of p16^{INK4a} which impaired cardiac function and tissue repair. These data suggest that CNPY2 is an important regulator of p16^{INK4a} and promotes cell proliferation and tissue repair through inhibition of the p16^{INK4a} pathway. CNPY2 treatment may offer a new approach to restore cardiac function after an MI.

1. Introduction

In a screen for hypoxia-regulated genes that encode secreted proteins, we discovered Canopy 2 (CNPY2), a HIF-1α-regulated secreted angiogenic growth factor [1]. CNPY2 encodes a member of the Canopy family of proteins (which includes CNPY1–4) and belongs to a larger protein superfamily called the saposin-like proteins (SAPLIPs) [2]. While only a few studies have evaluated the biological function of CNPY2 (alias putative secreted protein Zsig9, transmembrane protein 4, HP10390, and MIR-interacting saposin-like protein), published data support a role for this growth factor in directed cell growth and migration [3,4].

We recently showed that CNPY2 is widely distributed in tissues, with enriched expression in the heart, lung and liver [5]. Subsequently, we found that CNPY2 plays a critical role in the growth of colorectal cancer (CRC) by enhancing proliferation, migration and angiogenesis, and inhibiting apoptosis of CRC cells possibly through suppression of p53 activity [6]. In human smooth muscle cells (SMCs), the CNPY2 protein co-localized with the endoplasmic reticulum and Golgi and secreted CNPY2 was detected in the medium of cultured SMCs. CNPY2 stimulation activated cell division control protein 42 homolog (Cdc42), p21-activated kinase 1, and focal adhesion kinase in SMCs, resulting in

* Corresponding author at: PMCRT, 101 College St, Room 3-702, Toronto M5G 1L7, ON, Canada.
E-mail address: renkeli@uhnresearch.ca (R.-K. Li).

https://doi.org/10.1016/j.yjmcc.2019.04.018
Received 13 September 2018; Received in revised form 14 February 2019; Accepted 18 April 2019
Available online 29 April 2019
0022-2828/

enhanced proliferation, migration and tissue revascularization [1]. Using transgenic (TG) mice that overexpress human CNPY2, we found that CNPY2 promoted early-stage beneficial hypertrophic responses and prevented the later stages of ventricular dilatation possibly through decreased p53 activation and better maintained expression of the p53 target HIF-1α [7]. These results suggest that CNPY2 may be a useful component of angiogenic therapy to prevent the switch from beneficial compensatory hypertrophy to adverse ventricular dilatation and eventual heart failure. However, the potential beneficial effects of CNPY2 in ischemic heart attack have not been explored.

Despite great improvement in our understanding and treatment of ischemic heart disease, acute myocardial infarction (MI) remains a leading cause of mortality and morbidity [8]. The reparative response after MI can typically be divided into three phases: an inflammatory phase involving infiltration of neutrophils and monocytes to remove damaged cells and tissue, a proliferative phase associated with neovascularization and proliferation and differentiation of fibroblast-like cells, and a maturation phase including extracellular matrix synthesis leading to scar formation [9]. Cell proliferation plays an important role in cardiac repair, and involves endothelial cell, smooth muscle cell and fibroblast proliferation [10,11].

$P16^{INK4a}$, the first member of the INK4 family, has been suggested to play an important role in tumor growth suppression and cell senescence [12,13]. However, few studies have evaluated its function in cardiac tissue. Meyer et al. found that $p16^{INK4a}$ was increased 20-fold in perivascular fibrotic areas of pressure-overloaded hearts compared with control subjects [14]. It has been reported that $p16^{Ink4a}$-positive cells contribute to cardiac aging and clearance of $p16^{Ink4a}$-positive cells attenuates age-related deterioration of heart through preserving the functionality of cardio-protective K_{ATP} channels [15]. However, the regulation and control of $p16^{INK4a}$ related to cardiovascular pathophysiology and cellular senescence have not been extensively evaluated.

Here, we evaluated CNPY2 levels during heart failure in humans and MI in mice. We delineated the $p16^{INK4a}$ pathway as the mediator and mechanism responsible for the beneficial effects of CNPY2 using *Cnpy2* knockout (KO) and TG mice. We postulated that CNPY2 may exert its beneficial effects on cardiac repair after MI through promoting cell proliferation. We showed that knockout of *Cnpy2* resulted in impairment of mainly leukocyte and endothelial cell proliferation and deterioration of cardiac function. Furthermore, we demonstrated that CNPY2 is an important regulator of $p16^{INK4a}$ and promotes cell proliferation and tissue repair through PDK1/Akt-mediated inhibition of the $p16^{INK4a}$/cyclin D1/Rb pathway.

2. Materials and methods

2.1. Human cardiac tissue collection

Human cardiac tissue was obtained from four independent patient donors with end-stage heart failure and four control patients with normal ventricular function after obtaining informed consent at Toronto General Hospital. The study protocol was approved by the Research Ethics Board of the University Health Network in accordance with the Declaration of Helsinki. End-stage heart failure patients with decompensated heart failure who required the insertion of a left ventricular assist device (LVAD) to support their failing circulation had a core of left ventricular (LV) muscle removed to insert the LVAD cannula into the ventricular apex. A segment of this discarded muscle was obtained and served as heart failure samples. Patients with normal ventricular function undergoing coronary bypass grafting had tissue removed from the right atrium. A portion of the right atrium is routinely removed to insert the cannula used for cardiopulmonary bypass. Both the LV apical and right atrial tissue are routinely removed during surgery. This tissue was used as control samples. Samples were divided into three portions: one for RNA extraction for real-time qPCR, one for protein extraction for ELISA, and one for immunostaining and confocal imaging. No significant difference was found in terms of age, gender, medication, and other comorbidities that may have had a significant impact on heart-derived cell function independent of heart failure status.

2.2. Knockout and TG mice

All animal procedures were approved by the University Health Network Animal Care Committee. All experiments were carried out according to the Guide for the Care and Use of Laboratory Animals (NIH, 8th Edition, 2011). We generated *Cnpy2* KO mice from mice with a C57BL/6 background. Details of the KO construct and its restriction analysis can be found in the Supplementary Methods. The information regarding *Cnpy2* TG mice was documented in our previously published paper [7]. In brief, *Cnpy2* TG mouse line was generated as cardiac-specific carrying human *Cnpy2* driven by the α-myosin heavy chain (α-MHC) promoter. The final construct was linearized and microinjected into one-cell C57BL/6 embryos that were transferred into the oviduct of pseudopregnant CD1 mice. In total, six founders were obtained and bred with wild-type C57BL/6 mice, and four independent transgenic lines were used for experiments.

2.3. Myocardial infarction and cardiac function measurement

The left coronary artery of mice was permanently ligated (LAD) to induce MI. During this procedure, mice were intubated and ventilated with 2% isoflurane (Pharmaceutical Partners of Canada Inc., Richmond Hill, ON, Canada). Mice were given buprenorphine (0.05 mg/kg) for analgesia. Cardiac function was measured with echocardiography before and 7, 14, 21, and 28 days after MI. Fractional shortening (FS), left ventricular internal diameter systolic (LVIDs), and left ventricular internal diameter diastolic (LVIDd) were measured from M-mode images obtained by left ventricular short-axis view. After the functional analysis was complete (28 days after MI), the hearts were arrested, perfused with 10% formalin, and fixed for 1 day in 10% formalin. The hearts were then cut into 1 mm sections and photographed for morphometry. A mouse heart matrix (Model # HSMS001-1, Zivic instrument) was used to section the hearts into coronal slices with thicknesses in increment of 1.0 mm to ensure that equivalent histological sections within the ventricle were compared. The size of the infarct was defined as the ratio (percentage) of scar length to the entire left ventricular circumference. Scar thickness was also measured. After planimetry, heart segments were embedded in paraffin, sectioned at a 10-μm thickness, and mounted on glass slides. Masson's trichrome staining was performed to confirm scar tissue in the left ventricular free wall as described by the manufacturer's specifications (Sigma).

2.4. Immunofluorescent staining and confocal microscopy

Heart tissue was obtained 1, 3, 4, 7, and 28 days after LAD ligation or sham surgery. The samples were processed for embedding in optimal cutting temperature (OCT) compound or paraffin depending on the purpose of staining. The hearts were fixed in 2% paraformaldehyde (PFA) for 24 h after they were adequately flushed with PBS, and then transferred to 0.5 M sucrose at 4 °C and kept in solution overnight. The hearts were then embedded with OCT, and 7-μm-thick frozen sections prepared. For immunofluorescent staining, the slides were incubated with either rabbit anti-CNPY2 (1:200, generated as described previously [5]) or mouse anti-$p16^{INK4a}$ (1:400, Abcam) at room temperature for 2 h. Incubation with respective Alexa 488 or 546 conjugated secondary antibodies (Invitrogen) or Wheat Germ Agglutinin (Invitrogen) was carried out at room temperature with light protection for 1 h. Alexa 555 conjugated wheat germ agglutinin was used to label connective tissue extracellular matrix. The nuclei were identified with DAPI (Sigma). The number of positive cells in three randomly-selected

high-power fields per slide was determined and averaged with a Nikon Eclipase Ti fluorescent microscope. The number of animals used for each experiment is indicated in the figure legends. An Olympus Fluoview 2000 laser scanning confocal microscope was used to confirm the co-localization of fluorescent signals.

To evaluate the proliferative ability of mouse hearts after MI, we performed the 5-bromo-2′-deoxyuridine (BrdU) labeling technique. BrdU (50 mg/kg; Sigma) was administered to the mice by intraperitoneal injection for 3 consecutive days (one day prior to, the same day, and one day after MI). Coronary artery ligation was performed 1 day later. In a second experiment, mice received a single injection of BrdU on day 3 post-MI. During this procedure, mice were intubated and ventilated with 2% isoflurane (Pharmaceutical Partners of Canada Inc., Richmond Hill, ON, Canada). Mice were given buprenorphine (0.05 mg/kg) for analgesia. Animals were sacrificed 3 days after ligation and hearts were obtained. Frozen tissue sections were prepared and stained for BrdU incorporation. For BrdU immunostaining, the tissue sections were first treated with 2 N HCl for 30 min (10 min at RT, 20 min at 37 °C) to expose the antigens and then permeabilized with 0.5% Triton X-100. Sections were incubated with rat anti-BrdU (1:80, Abcam) for 2 h in a humidified atmosphere. After incubation with the primary antibody, the slides were washed three times in PBS and incubated with an Alexa 568-conjugated goat anti-rat secondary antibody (Invitrogen) for 1 h at room temperature. The nuclei were identified with DAPI staining. The BrdU-positive cells were counted using ImageJ software (NIH, Bethesda, MD) and the percentage of BrdU-positive cells was calculated.

2.5. In vitro cell proliferation assay with CNPY2 recombinant protein treatment

Cardiac fibroblasts were isolated from WT littermates and *Cnpy2* KO mice as described previously [11]. The isolated fibroblasts were treated with recombinant CNPY2 protein (10 nM) for 48 h and pulse-chased with BrdU (10 μM) for 6 h. The cells were then fixed in PFA for 10 min and immunostained for the BrdU antibody as described in Section 2.4.

2.6. RNA, RT-PCR and real-time qPCR

Total RNA was isolated from heart tissue using Trizol reagent (Sigma). Reverse transcription was performed using SuperScript III from Invitrogen; 1 μg of total RNA served as the template for each reaction. For PCR amplification of cDNA, reactions were run in an Eppendorf MasterCycler. Samples were heated at 95 °C for 5 min, followed by 30 cycles of 95 °C for 30 s, 55 °C for 1 min, 72 °C for 1 min, and 72 °C for an extra 10 min at the end of amplification. The RT-PCR products were separated on 1% agarose gel containing ethidium bromide. Real-time qPCR amplification was performed using the GeneAmp PCR 9600 Thermocycler (Applied Biosystems) for 40 cycles at 95 °C for 15 s, and 60 °C for 1 min. cDNA was processed using the SensiFAST SYBR No-ROX Kit (Bioline) according to the manufacturer's protocol. All reactions were performed in triplicate. A melting curve was generated at the end of every run to ensure product uniformity. Relative expression was calculated by the comparative threshold cycle method and expressed as $2^{-\Delta\Delta Ct}$, where the average of control Ct was set as baseline. All primers were designed using qPCR assay design software (Integrated Device Technology). Primer pairs specific for mouse $p16^{INK4a}$ (forward: 5'-GTGCGATATTTGCGTTCCG -3'; reverse: 5'-TCTG CTCTTGGGATTGGC-3') and GAPDH (forward: 5'-CGGCACAGTCAAGG CCGAGAATGG-3'; reverse: 5'-TCATGGATGACCTTGGCCAGGGGG-3') were used. GAPDH was used as an endogenous reference to correct for differences in the amount of total RNA added to the reaction and to compensate for different levels of inhibition during reverse transcription of RNA and during PCR.

2.7. Protein isolation, enzyme-linked immunosorbent assay (ELISA) and western blotting

To determine protein levels, heart samples were separated into scar and remote (normal muscle) regions and homogenized in liquid N_2. The total protein was extracted from powdered tissue in lysis buffer (20 mM Tris [pH 7.4], 150 mM NaCl, 1 mM EDTA, 1 mM EGTA, 1% Triton, 2.5 mM Na pyrophsphate, 1 mM β-glycerolphosphate, 1 mM Na3VO4, 1 μg/ml of leupeptin, 1 μg/ml of pepstatin, and 1 mM phenylmethylsulfonyl fluoride) for 1 h on ice. After centrifugation at 10,000*g* for 10 min, the supernatant was collected and protein concentration was measured using a Bio-Rad DC protein assay kit. The level of CNPY2 was determined using ELISA as described previously [5] and normalized by pg/mg total protein.

For Western blotting, denatured protein samples (50 μg) were fractionated through a 4% stacking and 10% running SDS-PAGE gel, and the fractionated proteins were transferred to a PVDF membrane. Blots were blocked for 1 h at room temperature with blocking buffer. The primary antibodies (rabbit anti-CNPY2, rabbit anti-cyclin D1, phospho-Ser807/811-Rb, total Rb, phospho-ser473-Akt, total Akt, phospho-Ser241-PDK1, total PDK1, mouse anti- cyclin-dependent kinases [CDK] 6, all from Cell Signaling Technology, rabbit anti-CDK4 from Santa Cruz) were reacted with the blots overnight at 4 °C. After washing (3× 5 min in 1× TBS-0.1% Tween 20), the blots were incubated with horseradish peroxidase-conjugated secondary antibody at 1:2000 dilution for 1 h at room temperature. The specific proteins were detected by chemiluminescence substrate. For quantification, densitometry of the target bands was divided by the corresponding densitometry of the GAPDH (Millipore) band.

2.8. Flow cytometry

Mouse hearts were collected 3 or 4 days post-MI, and separated into the injured and non-injured segments. The infarcted segments were minced and digested using 0.1% collagenase type II (Worthington, Lakewood, NJ, USA) at 37 °C for 30 min. After filtering through a 100 μm filter, the cells were washed and resuspended in FACS buffer (2% BSA-PBS). Cells were stained with either goat anti-DDR-2 (Clone N-20; Santa Cruz, Cat#: SC-7555), APC anti-mouse CD31 (Clone: MEC13.3; Biolegend, Cat#:102509), APC anti-mouse CD45 (Clone: 30-F11; Biolegend, Cat#:103112) respectively. All antibody incubation was carried out for 30 min at 4 °C in the dark. Alexa633-conjugated donkey anti-goat (Invitrogen, 1:200) was added for staining with mouse DDR-2. Proliferative cells were identified using the FITC BrdU Flow Kit according to the manufacturer's instructions (BD biosciences). Fluorescent minus 1 as negative controls (FMOs) were used for gating of $BrdU^+$ cells. Flow cytometry was performed using a LSRII flow cytometer (BD Biosciences). Data were analyzed using FlowJo (TreeStar).

2.9. Statistical analysis

All values are presented as mean ± SEM. Statistical analyses were performed using GraphPad Prism 7 (GraphPad, La Jolla, CA). A two-tailed Student's *t*-test was used for two-group comparisons. Comparisons of parameters among 3 or more groups were analyzed using one-way analysis of variance (ANOVA) or two-way ANOVA with repeated measures followed by Newman-Keuls *post-hoc* tests. Differences were considered statistically significant at $p < .05$.

3. Results

3.1. Decreased CNPY2 expression during heart failure in humans and cardiac injury in mice

CNPY2 expression was evaluated in cardiac tissue from patients with end-stage heart failure and control patients with normal

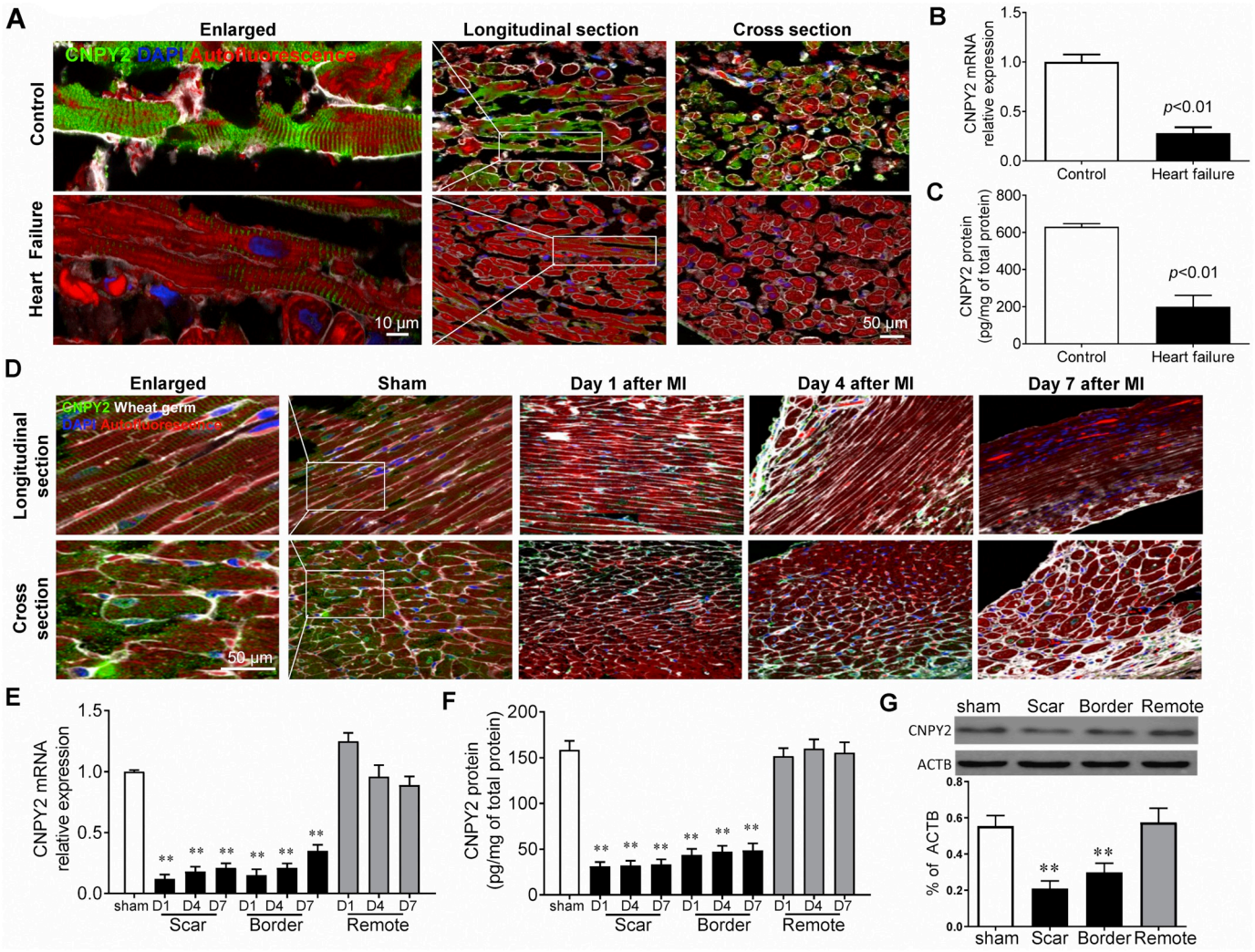

Fig. 1. Loss of endogenous CNPY2 during heart failure in humans and MI in mice.
Immunofluorescence staining **(A)**, real-time qPCR **(B)** and enzyme-linked immunosorbent assay **(**ELISA, **C)** showed that endogenous CNPY2 was significantly lower in myocardial tissue from patients with end-stage heart failure than control patients with normal ventricular function (n = 4/group). **(D)** Representative images of immunolabeling of CNPY2 in sham and infarcted mouse hearts. CNPY2 mRNA (**E**, measured by real-time qPCR) and protein (**F**, measured by ELISA) expression levels were significantly decreased in the scar and border zones from Day 1 to 7 following myocardial infarction (MI) compared to sham control mice (**$p < .01$, n = 5/group). (**G**) Western blot analysis showed that CNPY2 protein levels were significantly decreased in the scar and border zones at Day 4 post MI compared to sham control mice. (**$p < .01$, n = 5/group). CNPY2: Canopy 2.

ventricular function by three means: immunofluorescence staining (Fig. 1A), real-time qPCR (Fig. 1B) and ELISA (Fig. 1C). As shown in Fig. 1A, the heart tissue from patients with end-stage heart failure had less CNPY2 expression compared with control patient samples. This result was confirmed by real-time qPCR detection, and showed that myocardial tissue from heart failure patients had significantly lower endogenous CNPY2 mRNA levels than that from control patients (Fig. 1B). To determine if these findings hold true in mice, sham and infarcted mouse hearts were immunolabeled for CNPY2 which showed less CNPY2 staining in the scar/border area of infarcted hearts at 1, 4, and 7 days post MI compared with control sham hearts (Fig. 1D). Moreover, similar to that observed in human participants, CNPY2 mRNA (Fig. 1E) and protein (Fig. 1F) expression in mouse hearts decreased significantly following MI. This finding was also confirmed by Western blot analysis (Fig. 1G). These results indicate that cardiac injury and progressive heart failure were associated with decreased CNPY2 levels in both humans and mice.

3.2. Impaired cardiac function after MI in Cnpy2 KO mice

To further elucidate the role of CNPY2 under the pathological condition of MI, we generated *Cnpy2* KO mice using the C57BL/6 background (Supplementary Fig. 1). KO mice and their WT littermates were distinguished by tail genomic DNA genotyping PCR (Supplementary Fig. 1C). The loss of CNPY2 protein expression in the KO mice was also confirmed by Western blot (Supplementary Fig. 2). KO mice showed no noticeable difference in general morphology or baseline cardiac function except having slightly lower body weight compared to WT mice at all ages (Supplementary Fig. 3). MI was induced in both KO and WT littermates and cardiac function was determined by echocardiography. Representative M-mode echocardiographic images were taken 28 days post MI (Fig. 2A). Fractional shortening (FS, Fig. 2B) and ejection fraction (Fig. 2C) were similar between WT and KO mice before MI, while both parameters in KO mice were significantly lower 2 weeks after MI and these effects were

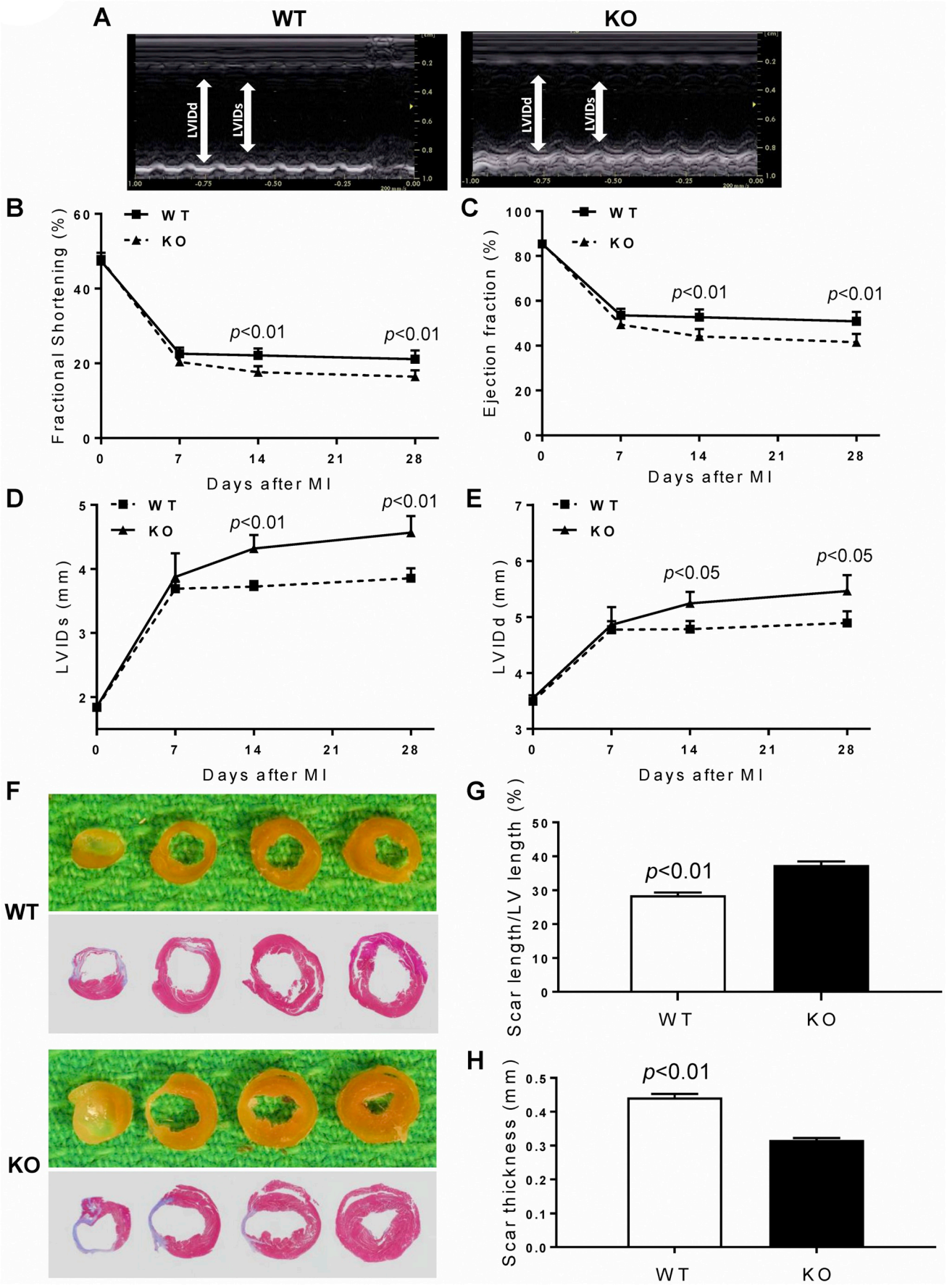

(caption on next page)

Fig. 2. Impaired cardiac function after MI in *Cnpy2* KO mice.
(A) Representative M-mode echocardiographic images taken 28 days post myocardial infarction (MI) in mice. Decreased fractional shortening **(B)** and ejection fraction **(C)**, increased left ventricular internal diameter systolic (LVIDs, **D**) and left ventricular internal diameter diastolic (LVIDd, **E**) were observed at 14 days post MI and were sustained up to 28 days post MI in *Cnpy2* KO mice compared to WT mice (n = 7–9/group). Morphological analysis and Masson's trichrome staining of hearts indicated that scar size **(F, G)** was significantly increased and scar thickness **(H)** was significantly reduced in *Cnpy2* KO mice compared to WT mice (n = 7/group). CNPY2: Canopy 2; WT: wild-type; KO: knockout.

sustained for up to 4 weeks. Left ventricular internal diameter end systole (LVIDs, Fig. 2D) and end diastole (LVIDd, Fig. 2E) were also significantly higher in KO compared to WT mice starting 2 weeks after MI. Morphological analysis and Masson's trichrome staining of hearts indicated that scar size (Fig. 2F–G) was significantly increased and scar thickness (Fig. 2H) was significantly reduced in *Cnpy2* KO mice compared to WT mice. These data suggest that knockout of *Cnpy2* contributed to progressive adverse cardiac remodeling after MI.

3.3. Decreased cell proliferation in Cnpy2 KO mice is associated with increased p16 ^{INK4a} expression

Previously, we showed that CNPY2 is a strong stimulator of cell proliferation [1,6], and thus postulated that CNPY2 may exert its protective effect on cardiac repair after MI through promoting cell proliferation. To determine the effect of CNPY2 on cell proliferation, BrdU pulse chasing was performed and WT and KO mice received BrdU injections for 3 days (one day prior to, one day at, and one day after MI, Fig. 3A). Heart samples from sham or infarcted mice were collected 3 days post MI. Immunolabeling of BrdU revealed a greater number of BrdU$^+$ cells in the border and infarct regions compared with sham-operated hearts or the remote area in both KO and WT groups (Fig. 3B). However, the number of proliferative cells was significantly lower in the border and infarct regions of KO than WT hearts (Fig. 3B).

We previously determined that CNPY2 may stimulate cell proliferation through suppression of p53 activity [6]. On the other hand, p16^{INK4a} is well known as a negative regulator of the cell cycle in vitro and in vivo [16,17]. Overexpression of p16^{INK4a} induces the inhibition

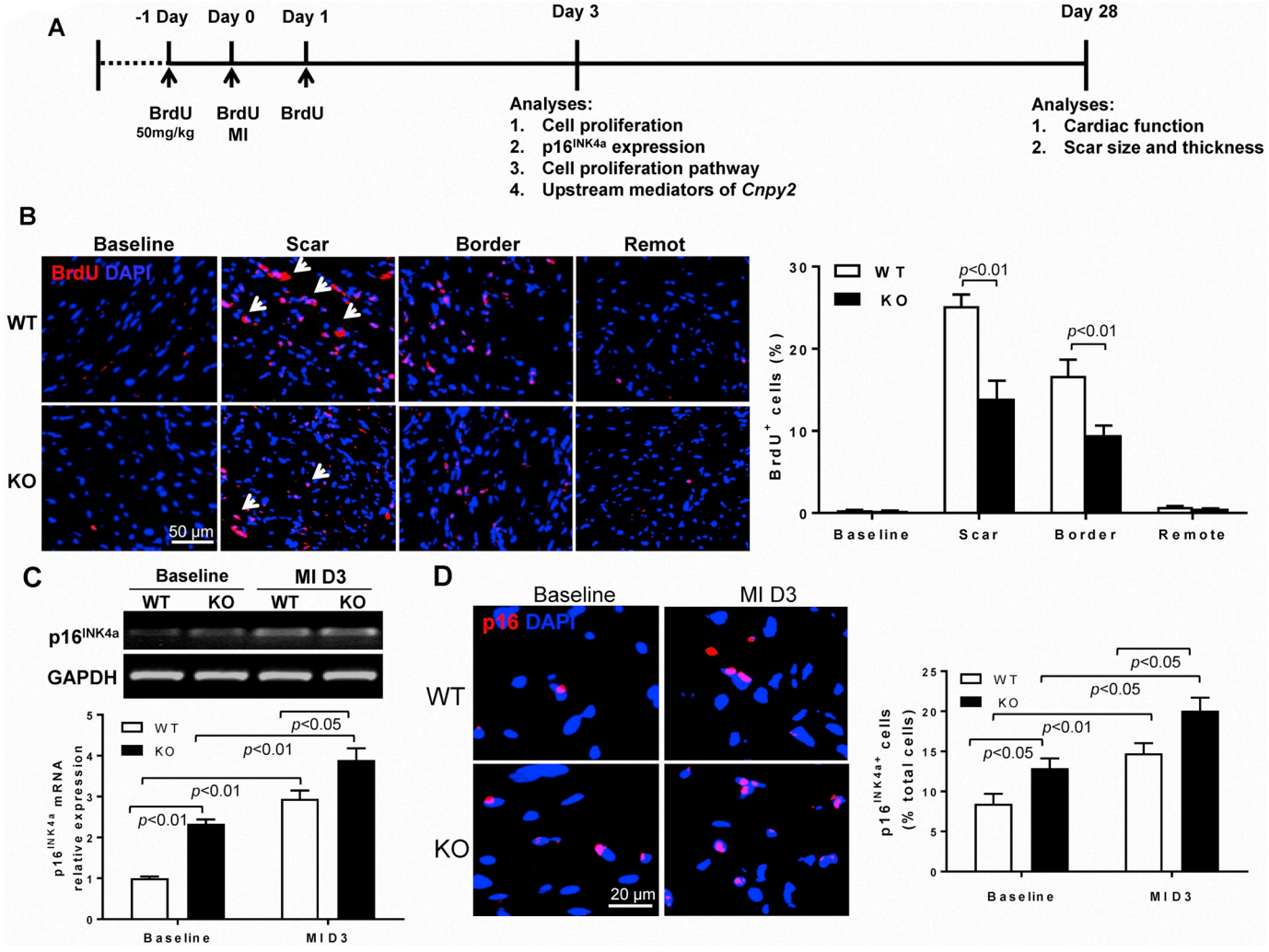

Fig. 3. Decreased cellular proliferation in *Cnpy2* KO mice was associated with increased p16^{INK4a} expression.
(A) Cell proliferation in WT and *Cnpy2* KO mice at baseline and at 3 days after myocardial infarction (MI) was assessed by 5-Bromo-2′-deoxyuridine (BrdU) pulse chasing. **(B)** After MI, the number of BrdU$^+$ cells was significantly lower in the scar and border zones of hearts from *Cnpy2* KO than WT mice (n = 4/group). **(C)** Real-time qPCR revealed significantly increased p16^{INK4a} mRNA levels in the hearts of *Cnpy2* KO than WT mice both at baseline and at 3 days after MI (n = 4/group). **(D)** Immunofluorescence staining confirmed a significantly greater number of p16^{INK4a+} cells both at baseline and at 3 days after MI in *Cnpy2* KO hearts compared to WT hearts (n = 4/group). CNPY2: Canopy 2; WT: wild-type; KO: knockout.

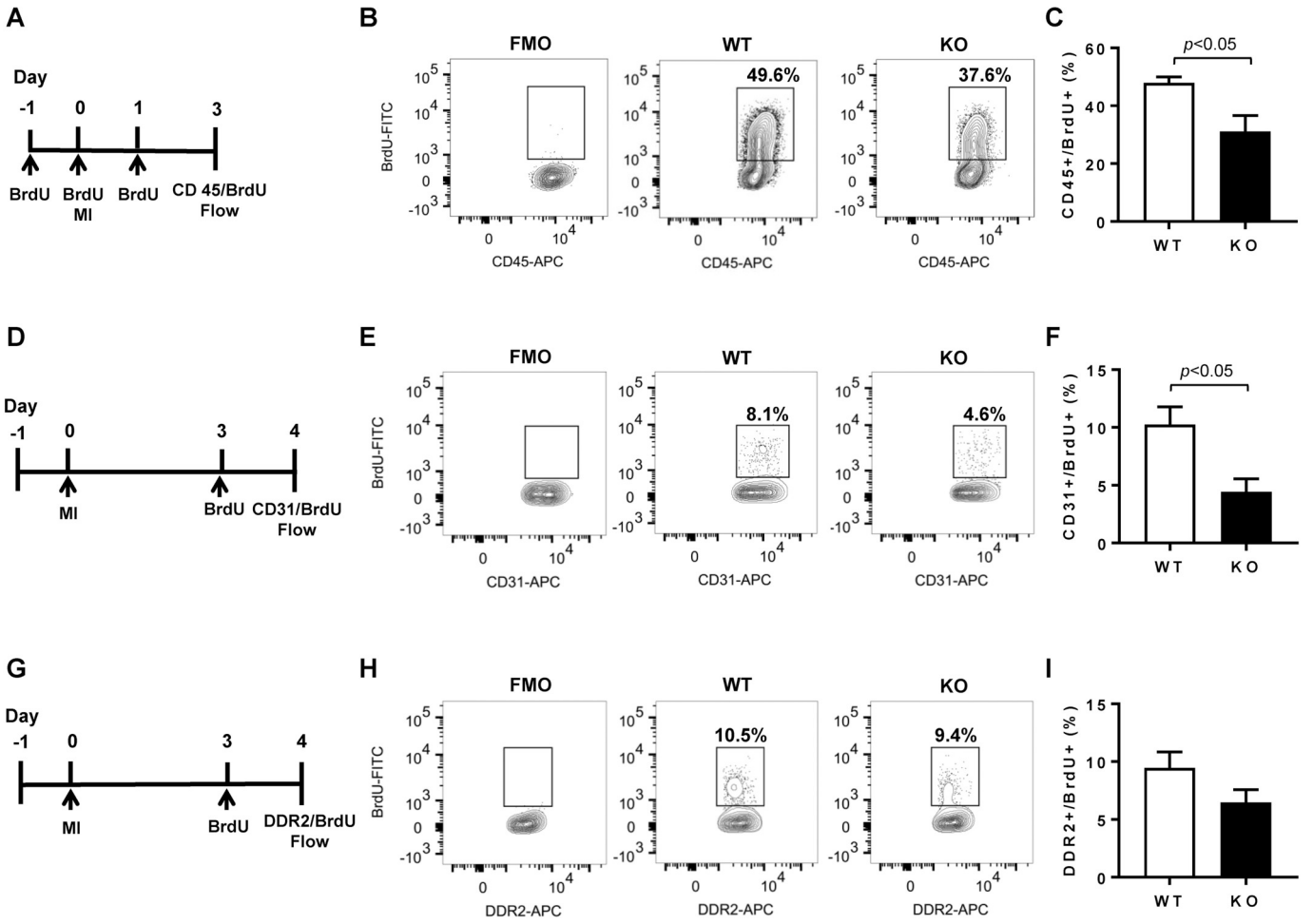

Fig. 4. Knockout of *Cnpy2* impaired leukocyte and endothelial cell proliferation.
(**A**) Mice were injected with 5-Bromo-2′-deoxyuridine (BrdU) 3 times (one day before, the day of, and one day after MI) and leukocyte (CD45) proliferation was assessed by BrdU staining and flow cytometry on day 3 post-MI. (**B**) Representative flow cytometry plots of $CD45^+/BrdU^+$ cells from WT and *Cnpy2* KO hearts. (**C**) Quantification of $CD45^+/BrdU^+$ cells, $n = 4$/group. (**D**) Mice were injected with BrdU on day 3 post-MI and hearts collected for flow cytometry on day 4 to assess endothelial ($CD31^+$) cell proliferation. (**E**) Representative flow cytometry plots of $CD31^+/BrdU^+$ cells from WT and *Cnpy2* KO hearts. (**F**) Quantification of $CD31^+/BrdU^+$ cells, $n = 5$/group. (**G**) Mice were injected with BrdU on day 3 post-MI and hearts collected for flow cytometry on day 4 to assess fibroblast ($DDR2^+$) proliferation. (**H**) Representative flow cytometry plots of $DDR2^+/BrdU^+$ cells from WT and Cnpy2 KO hearts. (**I**) Quantification of $DDR2^+/BrdU^+$ cells, n = 5/group. Representative FMOs (fluorescent minus 1 as negative controls) used for gates are shown for each marker. CNPY2: Canopy 2; WT: wild-type; KO: knockout; MI: myocardial infarction.

of cell proliferation, which has mainly been considered to result from arrest in the G1 phase of the cell cycle. Considering the important roles of p53 and $p16^{INK4a}$ in cell proliferation, we first evaluated p53 and $p16^{INK4a}$ mRNA expression in the KO and WT hearts at baseline. To our surprise, we found the upregulation of $p16^{INK4a}$ mRNA to be more robust than that of p53 in KO compared with WT mice (Supplementary Fig. 4). Next, we further examined $p16^{INK4a}$ expression in WT and KO hearts both at baseline and 3 days after MI. As shown in Fig. 3C, $p16^{INK4a}$ mRNA was significantly higher in the hearts of *Cnpy2* KO than WT mice both at baseline and 3 days after MI. To evaluate $p16^{INK4a}$ protein expression, immunofluorescence staining was performed. Similarly, the number of $p16^{INK4a+}$ cells was significantly greater in *Cnpy2* KO hearts than WT hearts (Fig. 3D). These results suggest that the decreased cellular proliferation found in *Cnpy2* KO mice may be associated with increased $p16^{INK4a}$ expression.

Next, to determine the identity of the proliferating cells that were affected in *Cnpy2* KO hearts, we assessed BrdU incorporation using flow cytometry. Mice were injected with BrdU for 3 days (one day prior to, one day at, and one day after MI; Fig. 4A) after which leukocyte (CD45), proliferation was assessed. *Cnpy2* KO mice exhibited a reduction in leukocyte proliferation post-MI, as shown by significantly lower $CD45^+/BrdU^+$ cells in the infarcted myocardium compared to WT hearts (Fig. 4B and C). This data suggests that proliferation of bone marrow cells in response to MI is impaired in *Cnpy2* KO mice. In order to assess endothelial ($CD31^+$) and fibroblast ($DDR2^+$) proliferation, we used a second protocol to label cells which typically initiate proliferation after the early inflammatory phase post-MI. Mice were injected with BrdU on day 3 and hearts collected on day 4 post-MI (Fig. 4D). Consistent with impaired proliferative responses, *Cnpy2* KO mice exhibited a significant reduction in endothelial cell proliferation as $CD31^+/BrdU^+$ cells were lower in *Cnpy2* KO hearts compared to WT hearts (Fig. 4E and F). Examination of fibroblast proliferation revealed no significant difference between WT and *Cnpy2* KO hearts, however fibroblast proliferation was slightly lower in *Cnpy2* KO hearts (Fig. 4G–I). Collectively these results demonstrated that a loss of *Cnpy2* mainly impaired leukocyte and endothelial cell proliferation in response to MI.

3.4. Knockout of Cnpy2 activated $p16^{INK4a}$/cyclin D1/Rb pathway

$p16^{INK4a}$ exerts its cell proliferation inhibitory effects primarily by suppressing the activity of the cyclin D1-CDK4/6 complex and

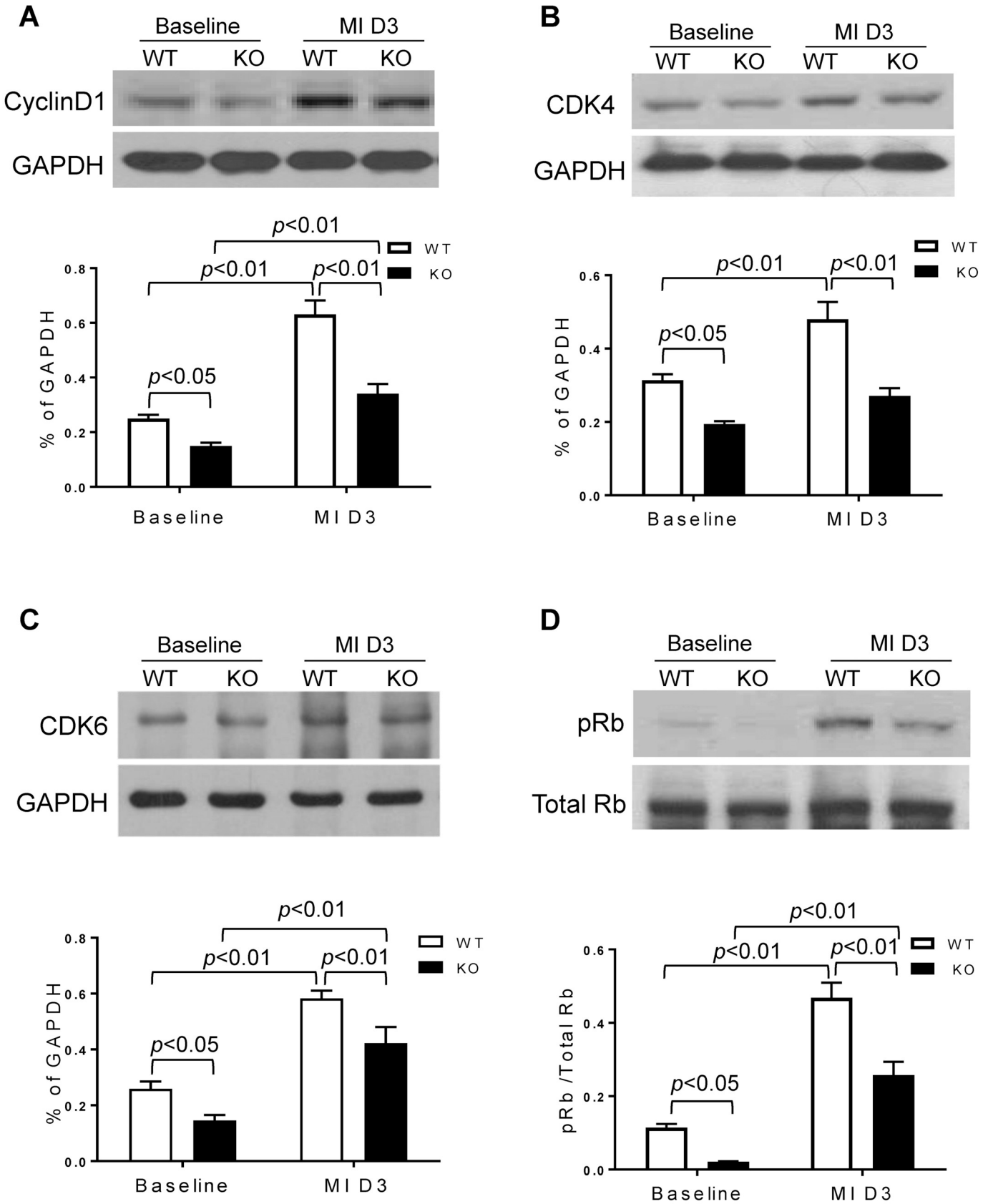

Fig. 5. Knockout of *Cnpy2* activated the $p16^{INK4a}$/cyclin D1/Rb pathway.
Western blots were performed to evaluate the protein expression of $p16^{INK4a}$/cyclin D1/Rb pathway molecules in the hearts of WT and KO mice in response to myocardial infarction (MI). Expression of cyclin D1 (**A**, n = 4/group), CDK 4 (**B**, *n* = 6/group), CDK6 (**C**, n = 4/group), and phospho-Rb (pRb, **D**, n = 3/group), the downstream mediators of $p16^{INK4a}$, was significantly decreased in *Cnpy2* KO mice compared to WT mice both at baseline and at 3 days after MI. CNPY2: Canopy 2; WT: wild-type; KO: knockout; CDK: cyclin-dependent kinase; Rb: retinoblastoma protein.

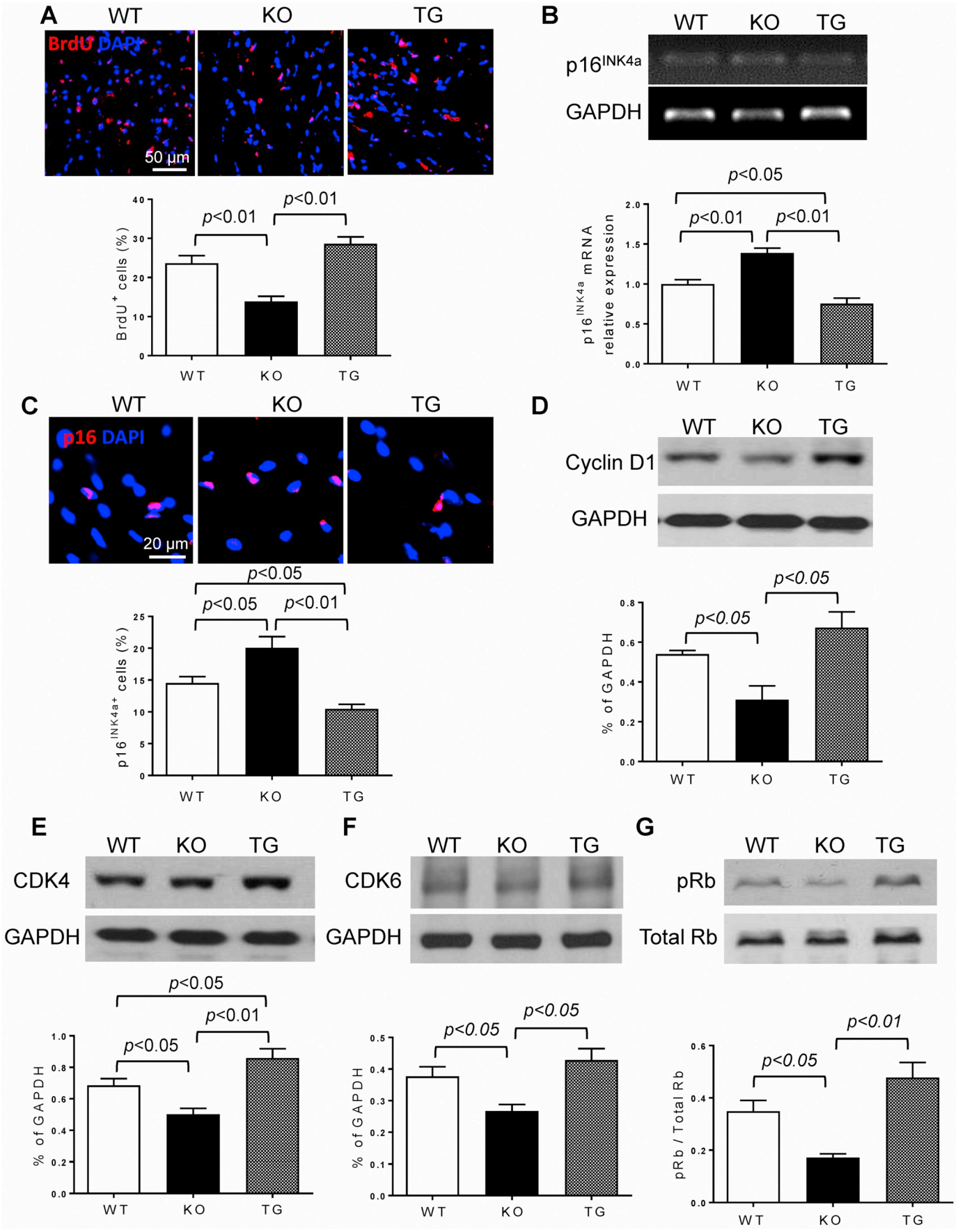

(caption on next page)

Fig. 6. Overexpression of CNPY2 reversed the inhibition of cell proliferation through deactivation of the $p16^{INK4a}$/cyclin D1/Rb pathway.
Cnpy2 transgenic (TG) mice were used to restore CNPY2 expression. Cell proliferation was assessed by 5-Bromo-2′-deoxyuridine (BrdU) pulse chasing. **(A)** The number of $BrdU^+$ cells in *Cnpy2* TG mice was significantly higher than in KO mice and was comparable to the number observed in WT mice at 3 days post myocardial infarction (MI, n = 4/group). The $p16^{INK4a}$ mRNA level (**B**, n = 4/group) and the number of $p16^{INK4a+}$ cells (**C**, n = 4/group) were significantly lower in *Cnpy2* TG mice than both KO mice and WT mice at 3 days post MI. Cyclin D1 (**D**, *n* = 3/group), CDK4 (**E**, n = 5/group), CDK6 (**F**, n = 3/group), and phospho-Rb (**G**, n = 4/group) protein expression was significantly higher in TG mice than KO mice and was comparable to expression in WT mice at 3 days post MI. CNPY2: Canopy 2; WT: wild-type; KO: knockout; CDK: cyclin-dependent kinase; Rb: retinoblastoma protein.

preventing retinoblastoma protein (Rb) phosphorylation [18]. To assess if the increased $p16^{INK4a}$ level in *Cnpy2* KO mice was associated with the activation of the $p16^{INK4a}$/cyclin D1/Rb pathway, the protein expression of this pathway was examined by Western blots. Our results revealed that increased $p16^{INK4a}$ expression was accompanied by reduced expression of cyclin D1 (Fig. 5A), CDK4 (Fig. 5B) and CDK6 (Fig. 5C) in KO mice both at baseline and after MI. A lower level of phospho-Rb (pRb) was induced by knockout of *Cnpy2* (Fig. 5D), whereas total Rb protein levels were not affected. These data suggest that loss of CNPY2 may contribute to decreased cell proliferation via activating the $p16^{INK4a}$/cyclin D1/Rb pathway.

3.5. CNPY2 overexpression increased cell proliferation via suppressing the $p16^{INK4a}$/cyclin D1/Rb pathway

To further confirm the role of CNPY2 in relation to the $p16^{INK4a}$ pathway and cell proliferation, *Cnpy2* TG mice which had cardiac over expression CNPY2 protein were used. CNPY*2* protein overexpression was confirmed in TG mice as compared to the WT littermates (Supplementary Fig. 2). MI was induced in WT, *Cnpy2* KO and TG mice and BrdU pulse chasing was conducted to evaluate cell proliferation. As expected, the percentage of $BrdU^+$ cells in *Cnpy2* TG mice was significantly higher than in KO mice and was similar to WT mice at 3 days post MI (Fig. 6A). Furthermore, $p16^{INK4a}$ mRNA expression and the percentage of $p16^{INK4a+}$ cells were significantly lower in *Cnpy2* TG mice compared to both KO mice and WT mice at 3 days post MI (Fig. 6B–C). On the other hand, the protein expression of cyclin D1 (Fig. 6D), CDK4 (Fig. 6E), CDK6 (Fig. 6F), and phospho-Rb (Fig. 6G) was significantly increased in TG mice compared to KO mice and was comparable to WT mice at 3 days post MI. These observations were further confirmed in an in vitro experiment with recombinant CNPY2 protein treatment. Treatment of cardiac fibroblasts isolated from *Cnpy2* KO mice with recombinant CNPY2 protein increased the number of $BrdU^+$ cells with a concomitant decrease in $p16^{INK4a}$ mRNA level (Supplementary Fig. 5). These results indicate that restoration of CNPY2 levels increased cell proliferation via inhibition of the $p16^{INK4a}$/cyclin D1/Rb pathway.

3.6. Knockout of Cnpy2 activated $p16^{INK4a}$/cyclin D1/Rb pathway through inhibition of PDK1/Akt pathway

Previously, we found that cardiomyocytes treated with recombinant CNPY2 protein led to the activation of Akt through phosphorylation of threonine308 (Thr308) in the activation loop by 3-phosphatidylinositol-dependent kinase-1 (PDK1). The PKB/Akt pathway plays a significant role in cell growth, proliferation, survival, protein synthesis, transcription, and apoptosis, and it is associated with $p16^{INK4a}$ inhibition [19]. To find the possible link between CNPY2-regulated $p16^{INK4a}$ suppression and the Akt signaling pathway, we evaluated the pathway molecules, phospho-PDK1 and phospho-Akt in the hearts of WT and KO mice in response to MI. Phospho-PDK1 and phospho-Akt were activated in the hearts of both WT and KO mice in response to MI (Fig. 7A–B). However, the levels of phospho-PDK1 and phospho-Akt were significantly lower in the hearts of *Cnpy2* KO than WT mice although the total PDK1 and AKT protein levels were unchanged between the groups. On the other hand, phospho-PDK1 and phospho-Akt levels in *Cnpy2* TG mice were completely restored to normal levels and comparable to WT mice (Fig. 7C–D). These results suggest that loss of CNPY2 may augment $p16^{INK4a}$ activity through inhibition of the PDK1/Akt pathway.

4. Discussion

After an MI, extensive cardiomyocyte necrosis and remodeling of the ventricular wall occurs. Fibroblasts and endothelial cells undergo rapid proliferation and migrate to the infarct zone where dead tissue is replaced with granulation tissue [11]. Endogenous repair responses to injury include scar healing and contraction, and augmentation of scar healing may inhibit the progress of heart failure after an extensive MI [11]. In this study, we found that CNPY2 was downregulated in the hearts of both end-stage heart failure patients and post-MI mice. The level of CNPY2 in mouse hearts was significantly downregulated from Day 1 to 7 after MI which corresponded to the stimulation of cardiac proliferation and the inflammatory response to the infarction. However, the decreased expression of CNPY2 may hamper cell proliferation and interfere with scar healing. To investigate the mechanisms associated with the beneficial effects of CNPY2, we used *Cnpy2* KO and TG (overexpressing) mice. In our in vivo MI mouse model, knockout of *Cnpy2* led to impaired cardiac function with thinning and expansion of the infarcted region. To some degree, the adverse effect of *Cnpy2* KO on scar healing and cardiac function was due to inhibition of early activation of cell proliferation, especially leukocyte and endothelial cell proliferation. Indeed, overexpression of CNPY2 in the cardiac tissue of transgenic mice reversed the inhibition of cell proliferation and improved tissue repair and scar healing. Some studies have also reported an effect of CNPY2 on cell proliferation, including malignant cells such as renal carcinoma cells and HCT116 human colorectal cancer cells [6,20]. Furthermore, Guo et al. reported that CNPY2 enhanced in vitro smooth muscle cell proliferation [1]. Our data suggest that CNPY2 is important for cellular proliferative capacity especially during the early proliferative phase of MI which is critical for tissue repair and scar healing.

Mechanistically, we found that knockout of *Cnpy2* triggers $p16^{INK4}$/cyclin D1/Rb signaling which in turn manifested its inhibitory effect on cell proliferation. The tumor suppressor gene $p16^{INK4a}$ is a member of the INK4 cell cycle proteins and has been shown to regulate G1 cell cycle progression by interfering with cyclin/CDK complexes. Activation of cyclin/CDK activity is required for cell cycle progression and G1/S transition in response to growth factor stimulation. The expression of cyclin D and CDK4/6 in the G1 cell cycle acts as the primary sensors of positive and negative environmental signals [21–23]. The cyclin D/CDK4/6 complexes induce the phosphorylation of Rb protein and the release of E2F, which trigger G1 cell cycle progression. Normally, Rb binds to the members of the E2F family of transcription factors. In response to the growth factors, the Rb protein is phosphorylated and dissociated from E2F, which triggers G1 cell cycle progression [24]. On the other hand, the upregulation of CDK inhibitors, such as $p21^{CIP1/WAF1}$ and $p16^{INK4a}$ are frequently responsible for the inhibition of G1 cell cycle progression and for withdrawal from the cell cycle [25–27]. $p16^{INK4}$ is capable of binding to CDK4, inhibiting the catalytic activity of the CDK4/cyclin D1 enzymes, thereby blocking DNA replication [28]. Our results showed significantly increased $p16^{INK4}$ expression in the hearts of *Cnpy2* KO mice compared to WT mice both at baseline and 3 days after MI. In response to the increased $p16^{INK4}$ level, cyclin D1, CDK4 and 6 and phospho-Rb protein levels were significantly decreased

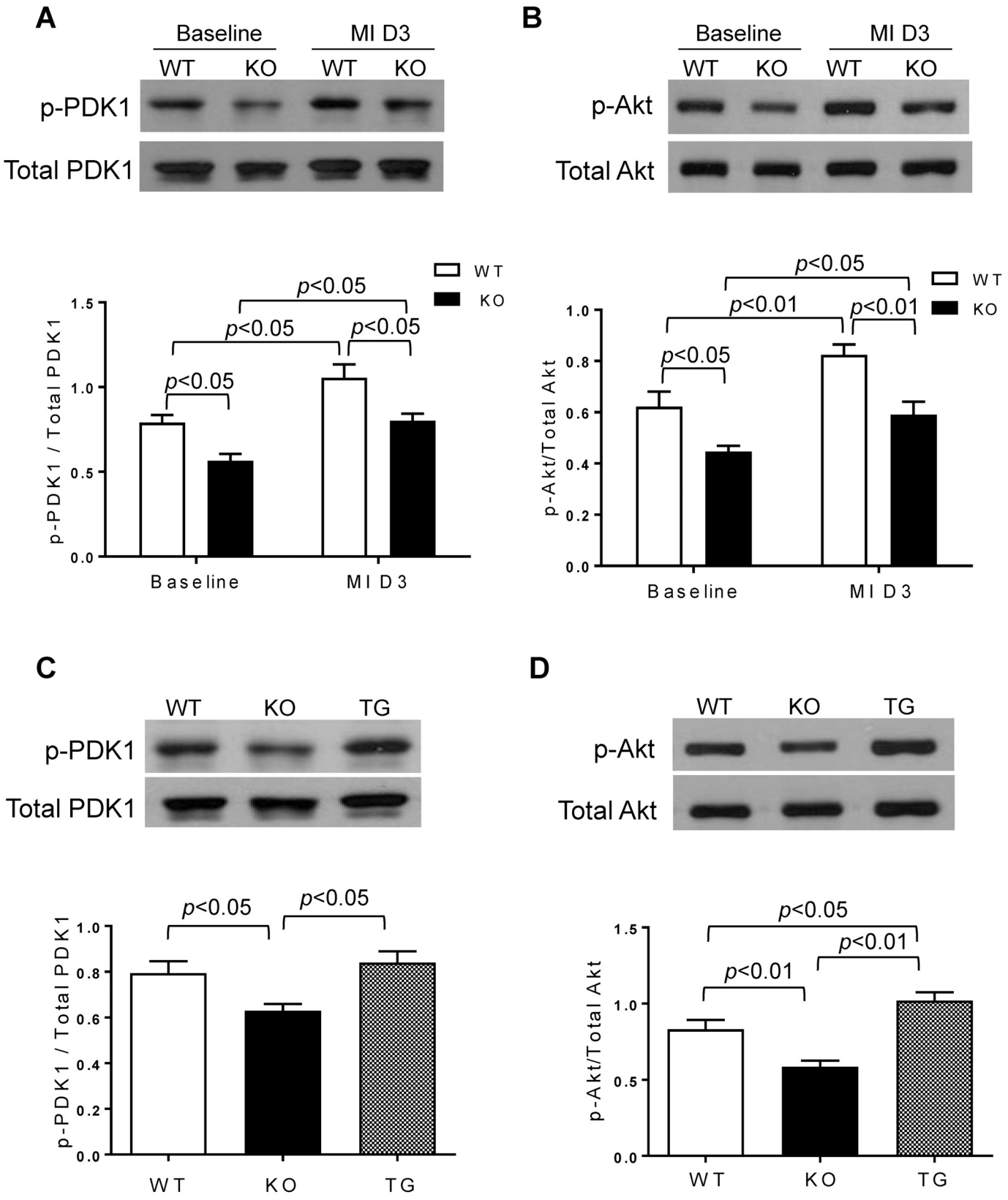

Fig. 7. Knockout of *Cnpy2* activated $p16^{INK4a}$ through inhibition of PDK1/Akt pathway.
The protein expression of upstream mediators of $p16^{INK4a}$, PDK1, and Akt was evaluated by Western blot in mouse hearts at 3 days post myocardial infarction (MI). Phospho-PDK1 (p-PDK1, **A**, n = 3/group) and phospho-Akt (p-Akt, **B**, n = 4/group) levels were significantly decreased in the infarcted hearts of *Cnpy2* KO mice compared to WT mice. p-PDK1 and p-Akt protein levels were completely restored to normal levels in the infarcted hearts of *Cnpy2* TG mice (**C, D**, n = 4/group). PDK1: 3-phosphatidylinositol-dependent kinase-1; CNPY2: Canopy 2; WT: wild-type; KO: knockout; TG: transgenic.

in *Cnpy2* KO mouse hearts. Conversely, the protein expression of cyclin D1, CDK4, CDK6 and phospho-Rb was significantly greater in TG mice than KO mice and was comparable to that of WT mice 3 days following MI. Combined, these results suggest that CNPY2 promotes cell proliferation and tissue repair through inhibition of the $p16^{INK4}$/cyclin D1/Rb pathway.

Members of the Akt family of serine/threonine protein kinases are critical regulators of multiple aspects of cell behaviour, including angiogenesis, metabolism, growth, proliferation, survival, protein synthesis, transcription, and apoptosis. Activation of PKB/Akt involves a phosphatidylinositol triphosphate (PIP3) generated by PI3K and a PH domain-dependent membrane translocation step, followed by phosphorylation of Thr308 in the activation loop within the kinase by PDK1 [29]. Phosphorylation of Thr308 partially activates Akt/PKB while phosphorylation of Akt at S473 in the carboxy-terminal hydrophobic motif, either by mTOR [30] or by DNA-PK [31], stimulates full Akt activity. Although Akt is best known for promoting cell survival and growth, Akt activation can also stimulate proliferation through multiple downstream targets impinging on cell-cycle regulation.

Although it hasn't been extensively investigated, researchers have suggested that there is a potential association between Akt and $p16^{INK4}$. Li et al. reported that caloric restriction regulates Akt/p70S6K1 signaling through SIRT1 which contributes to $p16^{INK4}$ suppression [19]. They demonstrated that Akt/p70S6K1 plays an important role in cell cycle and senescence regulation through inhibition of the $p16^{INK4}$/Rb pathway. Gao et al. found that the treatment of cells with LY-294002 markedly induced $p16^{INK4}$ expression in a dose-dependent manner, suggesting that LY-294002-induced G1 cell cycle arrest in ovarian cancer cells requires increased $p16^{INK4}$ expression [32]. Their data showed that the inhibition of PI3K/Akt/mTOR/p70S6K1 activities in the cells decreased the expression of Rb protein levels and induced the expression of $p16^{INK4}$. They contend that PI3K/Akt/mTOR regulates p70S6K1, which, in turn, mediates the $p16^{INK4}$/CDK4/cyclin D1/Rb pathway in G1 cell cycle progression in ovarian cancer cells. Consistent with these reports, our results revealed that the up-regulation of the $p16^{INK4}$/cyclin D1/Rb pathway by knockout of *Cnpy2* was accompanied by attenuation of PDK1/Akt activity. These data suggest that CNPY2 suppresses the $p16^{INK4}$ pathway possibly by activating the PDK1/Akt signaling pathway.

5. Conclusions

Here we show that CNPY2 plays an important role in heart injury repair and that the loss of CNPY2 leads to a decrease in cardiac reparative capacity and impaired functional recovery. This phenotype is characterized by diminished leukocyte and endothelial cell proliferation in the infarcted area. Reduced CNPY2 expression results in increased $p16^{INK4}$ activity which is mediated by inhibition of PDK1/Akt phosphorylation. Collectively, these results provide new insights into interactions between PDK1/Akt and the $p16^{INK4}$ pathway in CNPY2-induced cell proliferation and tissue repair that may contribute to the recovery of ischemic heart injury. CNPY2 may constitute a novel therapeutic target for ischemic heart disease.

Glossary

CDK: cyclin-dependent kinase
CNPY2: Canopy 2
KO: knockout
PDK1: 3-phosphatidylinositol-dependent kinase-1
Rb: retinoblastoma protein
TG: transgenic
WT: wild-type

Acknowledgements

We thank Dr. Leigh Botly for help with manuscript preparation and editing. FJA is a recipient of a Canadian Institutes of Health Research Postdoctoral Fellowship. This work was supported by the Canadian Institutes of Health Research [grant number 332652 to R-K.L.] and the Ontario Research Fund [grant number RE07-010 to R-K.L.]. R-K.L. holds a Tier 1 Canada Research Chair in Cardiac Regeneration.

Disclosures

The authors report no commercial or proprietary interest in any product or concept discussed in this article.

Appendix A. Supplementary data

Supplementary data to this article can be found online at https://doi.org/10.1016/j.yjmcc.2019.04.018.

References

[1] J. Guo, Y. Zhang, A. Mihic, S.H. Li, Z. Sun, Z. Shao, et al., A secreted protein (Canopy 2, CNPY2) enhances angiogenesis and promotes smooth muscle cell migration and proliferation, Cardiovasc. Res. 105 (2015) 383–393.
[2] H. Bruhn, A short guided tour through functional and structural features of saposin-like proteins, Biochem. J 389 (2005) 249–257.
[3] B.C. Bornhauser, P.A. Olsson, D. Lindholm, MSAP is a novel MIR-interacting protein that enhances neurite outgrowth and increases myosin regulatory light chain, J. Biol. Chem. 278 (2003) 35412–35420.
[4] B.C. Bornhauser, D. Lindholm, MSAP enhances migration of C6 glioma cells through phosphorylation of the myosin regulatory light chain, Cell. Mol. Life Sci 62 (2005) 1260–1266.
[5] K. Hatta, J. Guo, A. Ludke, S. Dhingra, K. Singh, M.L. Huang, et al., Expression of CNPY2 in mouse tissues: quantification and localization, PLoS One 9 (2014) e111370.
[6] P. Yan, H. Gong, X. Zhai, Y. Feng, J. Wu, S. He, et al., Decreasing CNPY2 expression diminishes colorectal tumor growth and development through activation of p53 pathway, Am. J. Pathol. 186 (2016) 1015–1024.
[7] J. Guo, A. Mihic, J. Wu, Y. Zhang, K. Singh, S. Dhingra, et al., Canopy 2 attenuates the transition from compensatory hypertrophy to dilated heart failure in hypertrophic cardiomyopathy, Eur. Heart J. 36 (2015) 2530–2540.
[8] Writing Group M, D. Lloyd-Jones, R.J. Adams, T.M. Brown, M. Carnethon, S. Dai, et al., Heart disease and stroke statistics–2010 update: a report from the American Heart Association, Circulation 121 (2010) e46–e215.
[9] M.B. Olsen, G.A. Hildrestrand, K. Scheffler, L.E. Vinge, K. Alfsnes, V. Palibrk, et al., NEIL3-dependent regulation of cardiac fibroblast proliferation prevents myocardial rupture, Cell Rep. 18 (2017) 82–92.
[10] M. Korf-Klingebiel, M.R. Reboll, S. Klede, T. Brod, A. Pich, F. Polten, et al., Myeloid-derived growth factor (C19orf10) mediates cardiac repair following myocardial infarction, Nat. Med. 21 (2015) 140–149.
[11] Y.S. Wang, S.H. Li, J. Guo, A. Mihic, J. Wu, L. Sun, et al., Role of miR-145 in cardiac myofibroblast differentiation, J. Mol. Cell. Cardiol. 66 (2014) 94–105.
[12] J. Gil, G. Peters, Regulation of the INK4b-ARF-INK4a tumour suppressor locus: all for one or one for all, Nat. Rev. Mol. Cell Biol. 7 (2006) 667–677.
[13] J. Krishnamurthy, C. Torrice, M.R. Ramsey, G.I. Kovalev, K. Al-Regaiey, L. Su, et al., Ink4a/Arf expression is a biomarker of aging, J. Clin. Invest. 114 (2004) 1299–1307.
[14] K. Meyer, B. Hodwin, D. Ramanujam, S. Engelhardt, A. Sarikas, Essential role for premature senescence of myofibroblasts in myocardial fibrosis, J. Am. Coll. Cardiol. 67 (2016) 2018–2028.
[15] D.J. Baker, B.G. Childs, M. Durik, M.E. Wijers, C.J. Sieben, J. Zhong, et al., Naturally occurring p16(Ink4a)-positive cells shorten healthy lifespan, Nature 530 (2016) 184–189.
[16] A. Oodi, M. Noruzinia, M. Habibi Roudkenar, M. Nikougoftar, M.S. Soltanpour, M. Khorshidfar, et al., Expression of P16 cell cycle inhibitor in human cord blood CD34+ expanded cells following co-culture with bone marrow-derived mesenchymal stem cells, Hematology 17 (2012) 334–340.
[17] A. Melk, B.M. Schmidt, O. Takeuchi, B. Sawitzki, D.C. Rayner, P.F. Halloran, Expression of p16INK4a and other cell cycle regulator and senescence associated genes in aging human kidney, Kidney Int. 65 (2004) 510–520.
[18] M. Serrano, G.J. Hannon, D. Beach, A new regulatory motif in cell-cycle control causing specific inhibition of cyclin D/CDK4, Nature 366 (1993) 704–707.
[19] Y. Li, T.O. Tollefsbol, p16(INK4a) suppression by glucose restriction contributes to human cellular lifespan extension through SIRT1-mediated epigenetic and genetic mechanisms, PLoS One 6 (2011) e17421.
[20] H. Taniguchi, S. Ito, T. Ueda, Y. Morioka, N. Kayukawa, A. Ueno, et al., CNPY2 promoted the proliferation of renal cell carcinoma cells and increased the expression of TP53, Biochem. Biophys. Res. Commun. 485 (2017) 267–271.
[21] J. Massague, S.W. Blain, R.S. Lo, TGFbeta signaling in growth control, cancer, and

heritable disorders, Cell 103 (2000) 295–309.
[22] C.J. Sherr, Cancer cell cycles, Science. 274 (1996) 1672–1677.
[23] C.J. Sherr, J.M. Roberts, CDK inhibitors: positive and negative regulators of G1-phase progression, Genes Dev. 13 (1999) 1501–1512.
[24] D.G. Johnson, R. Schneider-Broussard, Role of E2F in cell cycle control and cancer, Front. Biosci. J. Virtual Libr 3 (1998) d447–d448.
[25] D. Parry, S. Bates, D.J. Mann, G. Peters, Lack of cyclin D-Cdk complexes in Rb-negative cells correlates with high levels of p16INK4/MTS1 tumour suppressor gene product, EMBO J. 14 (1995) 503–511.
[26] I. Reynisdottir, K. Polyak, A. Iavarone, J. Massague, Kip/Cip and Ink4 Cdk inhibitors cooperate to induce cell cycle arrest in response to TGF-beta, Genes Dev. 9 (1995) 1831–1845.
[27] A. Swarbrick, C.S. Lee, R.L. Sutherland, E.A. Musgrove, Cooperation of p27(Kip1) and p18(INK4c) in progestin-mediated cell cycle arrest in T-47D breast cancer cells, Mol. Cell. Biol. 20 (2000) 2581–2591.
[28] S. Waga, G.J. Hannon, D. Beach, B. Stillman, The p21 inhibitor of cyclin-dependent kinases controls DNA replication by interaction with PCNA, Nature 369 (1994) 574–578.
[29] B.A. Hemmings, D.F. Restuccia, The PI3K-PKB/Akt pathway, Cold Spring Harb. Perspect. Biol. 7 (4) (2015).
[30] D.D. Sarbassov, D.A. Guertin, S.M. Ali, D.M. Sabatini, Phosphorylation and regulation of Akt/PKB by the rictor-mTOR complex, Science 307 (2005) 1098–1101.
[31] J. Feng, J. Park, P. Cron, D. Hess, B.A. Hemmings, Identification of a PKB/Akt hydrophobic motif Ser-473 kinase as DNA-dependent protein kinase, J. Biol. Chem. 279 (2004) 41189–41196.
[32] N. Gao, D.C. Flynn, Z. Zhang, X.S. Zhong, V. Walker, K.J. Liu, et al., G1 cell cycle progression and the expression of G1 cyclins are regulated by PI3K/AKT/mTOR/p70S6K1 signaling in human ovarian cancer cells, Am. J. Physiol. Cell Physiol 287 (2004) C281–C291.